Available online at www.sciencedirect.com
SCIENCE DIRECT
Journal of Sound and Vibration 293 (2006) 575–586
JOURNAL OF SOUND AND VIBRATION
www.elsevier.com/locate/jsvi

# Prediction of ground vibration from trains using the wavenumber finite and boundary element methods

X. Sheng, C.J.C. Jones*, D.J. Thompson

*Institute of Sound and Vibration Research, University of Southampton, Southampton SO17 1BJ, UK*

Accepted 26 August 2005
Available online 27 January 2006

**Abstract**

Ground vibration is an important aspect of the environmental impact of rail traffic. Vibration from about 2–200 Hz is caused by trains moving on the ground surface or in tunnels. The wave field thus created must be modelled in three dimensions because of the excitation under each axle and the movement of the train. For arbitrary geometry of structures and ground surface to be allowed in the analysis, numerical models are required. In most practical situations, the ground and built structures, such as tunnels and tracks, can be considered to be homogeneous in the track direction and may be modelled using the wavenumber finite/boundary element method which is formulated in terms of the wavenumber in that direction. Compared with a conventional, three-dimensional finite/boundary element model, this model is more computationally efficient and requires far less memory since discretization is only made over the vertical–transverse section of the ground and/or built structures. With this model it is possible to predict complete vibration spectra. In this paper, the wavenumber-based modelling approach is outlined and then the applicability of the method to surface vibration and tunnel vibration analyses is demonstrated.


## 1. Introduction

Ground vibration from surface and underground trains is an important issue for the railway industry. The frequencies of vibration cover a range from about 2–200 Hz [1]. Great efforts have been made in recent years to develop predictive models [2–5]. Previously, a semi-analytical wavenumber–frequency approach has been developed that assumes a flat, layered ground supporting a multiple-beam track model on which a train runs [4]. That model takes into account both vibration induced by the moving, quasi-static axle loads of the train and vibration excited dynamically as each axle runs over the irregular surface of the track. The prediction method can be extended to cases of arbitrary ground surface geometry or embedded structures, but an alternative to the flat layered ground model is required for the wave propagation problem. Numerical approaches such as the finite element method (FEM) and the boundary element method (BEM) must then be employed. A two-dimensional (2D) FE/BE model [6] and a three-dimensional (3D) FE/BE model [7] have been implemented. However, the 2D model cannot account for wave propagation in the direction of the track

*Corresponding author. Tel.: +44 2380 593224; fax: +44 2380 593190.
*E-mail address:* cjcj@isvr.soton.ac.uk (C.J.C. Jones).

0022-460X/$ - see front matter © 2006 Elsevier Ltd. All rights reserved.
doi:10.1016/j.jsv.2005.08.040

or the movement of the train. The 3D model, on the other hand, requires great computing resources and is complicated to use.

In many situations, the ground and built structures can be assumed to be homogeneous in the track direction. For such engineering configurations, an approach has been suggested [8] in which the problem is transformed into a sequence of 2D models depending on the wavenumber in the track direction. For each wavenumber, the finite cross-section of the built structure is modelled using FEM and the wave propagation in the surrounding soil is modelled using BEM. The FE and BE domains are coupled and the global FE/BE equations are then solved, giving the component of the response at that wavenumber. The actual response is then constructed from these components using an inverse Fourier transform. Since calculations are performed at discrete values of wavenumber, these methods may be termed the wavenumber FEMs/BEMs methods (but are also known as 'two-and-half dimensional' (2.5D) methods or 'generalized plane strain'). The simplicity and efficiency of this approach comes from the fact that the discretization is only made over the cross-section of the whole structure, and therefore the total number of degrees of freedom is greatly reduced compared with the corresponding (3D) model.

The wavenumber-based modelling approach is outlined briefly and then results are shown to demonstrate its applicability to different engineering cases. Three cases are considered: surface vibration where the track is on embankment, the effect on surface vibration of a stiffened layer of soil below the ground, also known as a 'wave impeding block' (WIB) (e.g. [9]), and vibration from a bored tunnel.

## 2. Wavenumber finite and boundary element methods

### 2.1. Finite element equation

Suppose an elastic body is infinitely long in the $x$-direction and its cross-sections are invariant with $x$. The cross-section at $x$, $A$, is discretized into a number of FEs. The same discretization is also made on the $x+\mathrm{d}x$ cross-section. An element area, $\mathrm{d}A$, on the $x$ cross-section and its counterpart on the $x+\mathrm{d}x$ cross-section define an element prism. The displacements of the $n$ nodes on the element $\mathrm{d}A$ are denoted by a $3n$ vector

$$\{\mathbf{q}(x,t)\} = (u_1, v_1, w_1, \ldots, u_n, v_n, w_n)^{\mathrm{T}}. \tag{1}$$

The corresponding nodal force vector is denoted by $\{\mathbf{F}(x,t)\}$. A shape function matrix of order $3\times 3n$ is defined and denoted by $[\mathbf{\Phi}(y,z)]$, so that the displacement vector of the element at any point $(x, y, z)$ may be approximated as

$$\{\mathbf{u}(x,y,z,t)\} = [\mathbf{\Phi}(y,z)]\{\mathbf{q}(x,t)\}. \tag{2}$$

Using Eqs. (1) and (2) to express the kinetic and potential energy of the element prism, and then inserting the energy expressions into the second Lagrange's equation, the differential equation of motion of the element is obtained as

$$[\mathbf{M}]\{\ddot{\mathbf{q}}(x,t)\} + [\mathbf{K}]_0\{\mathbf{q}(x,t)\} + [\mathbf{K}]_1\left\{\frac{\partial}{\partial x}\mathbf{q}(x,t)\right\} - [\mathbf{K}]_2\left\{\frac{\partial^2}{\partial x^2}\mathbf{q}(x,t)\right\} = \{\mathbf{F}(x,t)\}. \tag{3}$$

Expressions of the matrices in Eq. (3) can be found in Refs. [10–12]. Matrices $[\mathbf{M}]$, $[\mathbf{K}]_0$ and $[\mathbf{K}]_2$ are symmetric and $[\mathbf{K}]_1$ is anti-symmetric. Further, $[\mathbf{M}]$ and $[\mathbf{K}]_2$ are positive definite and $[\mathbf{K}]_0$ is non-negative.

The conventional 'assembly' of the element matrices in Eq. (3) can be applied to obtain the global matrices and global FE equation of the elastic body. The latter is still represented by Eq. (3). Now, by applying Fourier transforms

$$\bar{f}(\beta,t) = \int_{-\infty}^{\infty} f(x,t)\mathrm{e}^{-\mathrm{i}\beta x}\,\mathrm{d}x \tag{4}$$

and letting [12]

$$\bar{f}(\beta,t) = \tilde{f}(\beta)\mathrm{e}^{\mathrm{i}(\Omega-\beta c)t}. \tag{5}$$

Eq. (3) becomes

$$([\mathbf{K}]_0 + \mathrm{i}\beta[\mathbf{K}]_1 + \beta^2[\mathbf{K}]_2 - \omega^2[\mathbf{M}])\{\tilde{\mathbf{q}}(\beta)\} = \{\tilde{\mathbf{F}}(\beta)\}, \tag{6}$$

where it has been assumed that the nodal forces are all harmonic at radian frequency $\Omega$ and moving in the $x$-direction at speed $c$. $\omega$ is the equivalent frequency at wavenumber $\beta$, given by

$$\omega = \Omega - \beta c. \tag{7}$$

The transformed displacement vector $\{\tilde{\mathbf{q}}(\beta)\}$ can be determined from Eq. (6) for each $\beta$ and then the actual displacements are obtained using an inverse Fourier transform algorithm.

### 2.2. Boundary element equation

The BE equation is formed by the discretization of the integral equation for an elastic body [13]. Where the elastic body is infinitely long in the $x$-direction, so that the Fourier transform defined in Eqs. (4) and (5) can be applied, the integral formulation in terms of $\beta$, $y$ and $z$ can be derived as [12]

$$\begin{aligned}\delta_{kl}\tilde{u}_k(\beta, y_0, z_0) = &\int_\Gamma \tilde{p}_k(\beta, y, z)\tilde{u}^*_{kl}(-\beta, y, z; y_0, z_0)\,\mathrm{d}\Gamma - \int_\Gamma \tilde{p}^*_{kl}(-\beta, y, z; y_0, z_0)\tilde{u}_k(\beta, y, z)\,\mathrm{d}\Gamma \\ &+ \int_A \rho\tilde{b}_k(\beta, y, z)\tilde{u}^*_{kl}(-\beta, y, z; y_0, z_0)\,\mathrm{d}A,\end{aligned} \tag{8}$$

where $\Gamma$ is the boundary of the cross-section, $A$, of the elastic body in the $yz$-plane. Here, $\tilde{u}^*_{kl}(-\beta, y, z; y_0, z_0)$ and $\tilde{p}^*_{kl}(-\beta, y, z; y_0, z_0)$ denote the Fourier-transformed Green's functions for displacement and traction at $(y, z)$ due to a moving unit point load. The first subscript indicates the response direction (traction or displacement) while the second denotes the source direction. These Green's functions can be found in Ref. [14] for a stationary source (i.e. $c = 0$) and in Ref. [15] for a moving source. The boundary integral equation is established from Eq. (8) by taking point $(y_0, z_0)$ onto the boundary $\Gamma$. This reduces to the boundary integral equation in elasto-dynamics for a plane-strain problem when $\beta$ is set to zero.

The boundary integral equation is discretized using three-noded quadratic shape function BEs. This process is standard and finally gives the global BE equation

$$[\mathbf{H}]\{\tilde{\mathbf{u}}(\beta)\} = [\mathbf{G}]\{\tilde{\mathbf{p}}(\beta)\} + \{\tilde{\mathbf{B}}(\beta)\}, \tag{9}$$

where $[\mathbf{H}]$ and $[\mathbf{G}]$ are square matrices, $\{\tilde{\mathbf{u}}(\beta)\}$ and $\{\tilde{\mathbf{p}}(\beta)\}$ denote the nodal displacement vector and the nodal traction vector, and $\{\tilde{\mathbf{B}}(\beta)\}$ is formed from the last term in Eq. (8), the surface integral over $A$.

To evaluate matrices $[\mathbf{G}]$ and $[\mathbf{H}]$, integration along the boundary $\Gamma$ must be performed. When a collocation point $(y_0, z_0)$ is on an element along which integration is performed, the integrands become singular for both the evaluation of $[\mathbf{H}]$ and $[\mathbf{G}]$. The singular terms for constructing matrix $[\mathbf{G}]$ may be integrated after a treatment that takes into account the presence in the integrands of a weak singularity of logarithmic order. A commonly used method is to perform a nonlinear transformation with a vanishing derivative of the first order at the singular point so that the singularity in the integrands can be eliminated [16,17]. The singular terms for constructing matrix $[\mathbf{H}]$, however, are of higher order and are not integrable. The reason that the total integration round the boundary for these terms has a finite result is that the integrands are either a $\delta$-like function at the singular node or have singular terms of opposite signs either side of the node and these cancel. The implication of this is that the integral cannot be evaluated using any quadrature scheme on an element-by-element basis and an alternative method must be devised. In the case of a stationary harmonic load, the difficulty may be overcome by employing the rigid body motion technique combined with either a fully, or a locally enclosing elements technique [18]. For the moving load case a new technique has been implemented in Ref. [12].

Since the whole-space Green's functions are used, the ground surface and the horizontal interfaces of a layered ground must be truncated to form a BE model. The truncation may give significant errors to the calculated results near the edges of the model for a layered ground. A means has been designed which can greatly reduce this truncation effect [12]. This involves the use of special elements at the termination of the boundary that have been termed 'edge elements'.

### 2.3. Vibration power spectra

The FE equation and the BE equation derived above are coupled to form a single matrix equation relating displacements to forces. This is then solved for responses to moving harmonic loads of a single frequency. To produce results that are comparable with measured data, prediction is required of vibration spectra produced by rail roughness. To do so, the ground/built-structure system is further coupled with a vehicle model. In this study, a vehicle is represented by its unsprung masses plus the axle loads. This is reasonable since for frequencies higher than a few Hertz the effects of the car body and bogies are isolated by the primary suspension.

Ref. [4] gives a description of a method of coupling the vehicle to a coupled ground and track model in order to calculate the forces at the wheel/rail contacts. The relationship between vibration power spectra and 'roughness' power spectral density, derived in Ref. [4] for surface trains, is valid for any 2.5D structure interacting with a train. The wheel/rail contact force spectrum is calculated from the roughness wavenumber spectrum and the wheel, contact and rail receptances. In Ref. [4] the latter is calculated from the full track and ground model, this is appropriate for soft surface soils and for low frequency. However, for tunnel vibration at higher frequencies where the ground is stiffer and there is a stiff invert slab, a more efficient calculation of rail receptance can be carried out by assuming an infinitely stiff ground in a track model. Ref. [4] showed that the spectral response of the ground can be calculated from the the power spectral density of the rail irregularities at wavenumber $\beta_k$, $P_z(\beta_k)$, in $m^2$/(cycle/m) using the results of the track and ground model in terms of the vertical displacement spectrum of $(x, y, z)$ at frequency $f$ due to a unit vertical rail irregularity of wavenumber $\beta_k$. This is denoted and $S_w^0(x, y, z, f; \Omega_k)$ and has units of 1/Hz. The vertical displacement power spectrum produced by trains running uniformly at speed $c$ along a track is given by

$$P_w(x, y, z, f) = \frac{1}{2\pi}\sum_{k=1}^{\infty}[|S_w^0(x, y, z, f; \Omega_k)|^2 + |S_w^0(x, y, z, f; -\Omega_k)|^2]P_z(\beta_k)\Delta\beta + |S_w^0(x, y, z, f; 0)|^2, \quad (10)$$

where $P_w(x, y, z, f)$ is in units of $m^2/Hz^2$. At each wavenumber, the radian frequency of the generated wheel/rail forces is given by $\Omega_k = \beta_k c$. $\Delta\beta$ is the wavenumber spacing, in rad/m. $S_w^0(x, y, z, f; -\Omega_k)$ accounts for wavenumber $-\beta_k$ and for train speed $c \neq 0$ it is not equal to $S_w^0(x, y, z, f; \Omega_k)$. Finally, $S_w^0(x, y, z, f; 0)$ denotes the vertical displacement spectrum of point $(x, y, z)$ at frequency $f$ due to the moving axle loads of the train and gives the harmonic components of the excitation produced by the quasi-static passage of the axle loads. When divided by the time needed for the train to pass a fixed point, Eq. (10) gives the displacement power spectral density from which band-averaged vibration levels can be evaluated.

## 3. Applications

### 3.1. Vibration of a layered ground from surface trains

In the semi-analytical model for surface vibration [4], the embankment, if it exists, is modelled as an infinite beam. In the 2.5D FE/BE model, the embankment cross-section can be modelled using the FEM. Here, measured vibration is compared with a prediction from the 2.5D FE/BE model for the ETR500 train at a site called Via Tedalda in Italy [19]. Such a comparison with the semi-analytical model has previously been made in Ref. [20]. The vibration was measured at two points, 13 and 26 m from the track centre-line. Using Fig. 5 in Ref. [19], the ground is modelled as one layer of 10 m depth overlying a homogeneous half-space. The P- and S-wave speeds in the layer are identified as 995 and 300 m/s, and 1990 and 600 m/s in the half-space. In the absence of specific parameters, the track structure excluding the embankment has been assigned parameters typical of a ballasted track with monobloc sleepers (Table 1). The embankment is 2.7 m wide at the top, 4 m wide at the bottom and is 1.5 m high. Its density, Young's modulus and Poisson's ratio are estimated as 1800 kg/$m^3$, 20 MN/$m^2$ and 0.45. A model of five ETR500 passenger cars running at 25 m/s (90 km/h) is coupled with the track-ground system. The ground surface and the layer interface are each discretized using 50

Table 1
Parameters for the ballasted track

| | |
|---|---|
| Mass of rail beam per unit length of track (kg/m) | 120 |
| Bending stiffness of rail beam (N m$^2$) | $1.26 \times 10^7$ |
| Loss factor of the rail | 0.01 |
| Rail pad stiffness (N/m$^2$) | $3.5 \times 10^8$ |
| Rail pad loss factor | 0.15 |
| Mass of sleepers per unit length of track (kg/m) | 490 |
| Mass of ballast per unit length of track (kg/m) | 1200 |
| Ballast stiffness per unit length of track (N/m$^2$) | $3.15 \times 10^8$ |
| Loss factor of ballast | 1.0 |

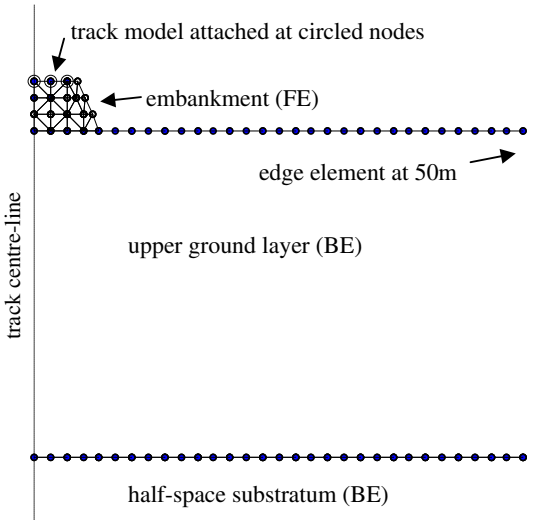


Fig. 1. Model of the Via Tedalda site.

three-noded BEs covering a lateral distance of 50 m from the track centre-line. At this distance each line of BEs is terminated with an 'edge element' [12]. Half the embankment is modelled using 23 three-noded triangular FEs. The model mesh is shown in Fig. 1. In the absence of specific data a typical rail vertical profile spectrum, shown in Fig. 2, has been used (the same as in Ref. [20]). In this and the two subsequent example analyses, no account is taken of the wheel's possible contribution to the roughness. The wheels are disc-braked in each case and so it is expected that the roughness at shorter wavelengths is less than that of the rails. At longer wavelengths the wheel would contribute to the excitation through 'out-of-roundness', however little information on typical values is known.

Figs. 3 and 4 show the predicted and measured vertical acceleration levels in the one-third octave bands from 1.6 to 80 Hz. Fig. 3, for the position at 13 m, shows good agreement between prediction and measurement for frequencies higher than 6.3 Hz. As for the prediction from the semi-analytical model [20], a discrepancy between the measurement and the 2.5D FE/BE model is also observed for frequencies between 2 and 5 Hz. Here the prediction gives levels much lower than those measured, which are themselves more than 70 dB down on the peak level. Comparison in this part of the spectrum may therefore not be appropriate. However, across the rest of the frequency range the prediction is more accurate than in Ref. [20], indicating that the ability to model the geometry and material of the embankment improves the model. Similar observations can be made for the comparison at 26 m.

The comparison presented here between the prediction and measurement validates the 2.5D FE/BE model. In fact the closeness of the results is better than for those of the model of Refs. [4,20].

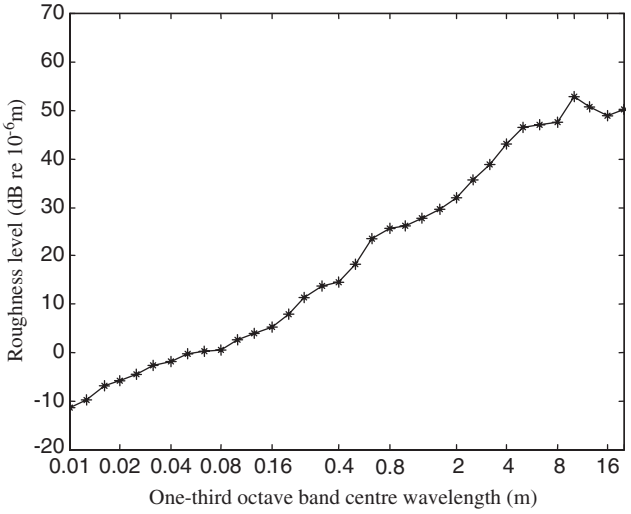


Fig. 2. Rail roughness level used in the predictions.

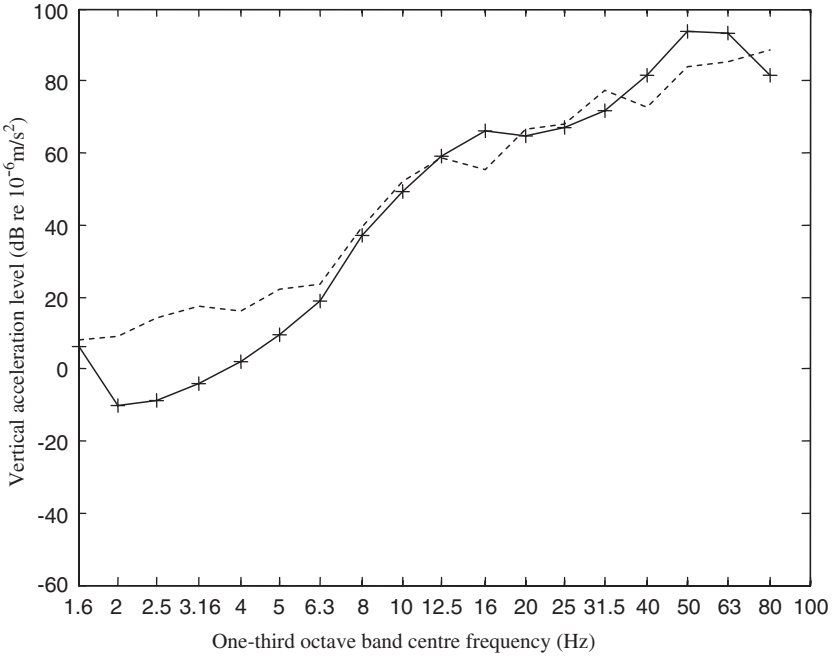


Fig. 3. Vertical acceleration levels at 13 m from the track at Via Tedalda when five ETR 500 cars run at 25 m/s. —, predicted; – – –, measured.

### 3.2. Vibration mitigation by a wave impeding block

Strong ground surface vibration occurs when a ground is soft and the train speed is close to the Rayleigh wave speed of the soil. To mitigate ground vibration, a stiffer plate may be inserted into the soil at a depth. This plate is called wave impeding block (WIB) in the literature (e.g. [9]). The mechanism of vibration mitigation is that the plate behaves like a rigid foundation to the upper layer of soil and wave propagation occurs in the upper layer only for frequencies higher than the cut-on frequency of the constrained upper layer. In other words, vibration at frequencies lower than the cut-on frequency can be expected to be mitigated by

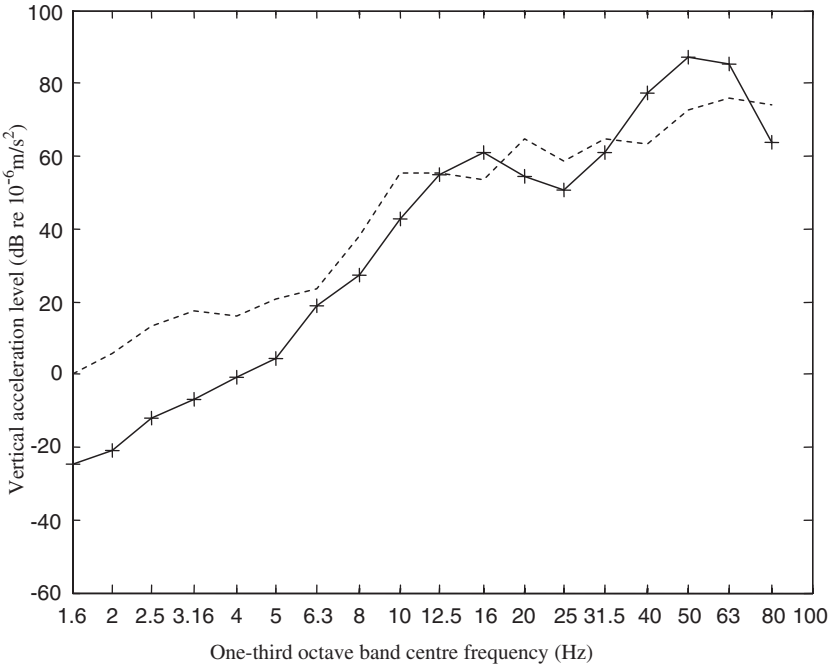


Fig. 4. Vertical acceleration levels at 26 m from the track at Via Tedalda when five ETR 500 cars run at 25 m/s. —, predicted; – – –, measured.

the WIB. The cut-on frequency may be estimated as $f_{\text{cut}} = c_2/4h$, where $h$ is the depth of the upper layer of soil and $c_2$ is its shear wave speed. This formula is exact only when the plate is rigid and extends to infinity in the horizontal plane.

A WIB could be constructed using concrete. This would provide a structure that would be much stiffer than the soil. However, the cost of removal and replacement of the track and soil would be very high. Instead, a WIB could be formed by 'jet grouting' without the need to remove the track. In this process cement-based grouts are injected into the ground using high-pressure erosive jets. Soil particles not removed become mixed with the grout to form a reinforced material. For predictions of the effectiveness of a WIB in a layered ground, numerical methods such as those presented in this paper must be used. Calculations are performed for a layered ground with parameters tabulated in Table 2. The track specified by Table 1 and the rail roughness spectrum defined in Fig. 2 is laid on the ground surface. A high-speed passenger coach [4] runs on the track at 60 m/s. The vertical velocity levels on the ground surface for the case without the WIB, have been predicted using the semi-analytical model [4] and are shown in Fig. 5 for three positions on the ground surface, i.e. 5, 10 and 20 m from the track centre-line. The predicted levels can be as high as 120 dB re $10^{-9}$ m/s for the position close to the track. The strong rise in the response between 6 and 20 Hz is due to the cut-on (13 Hz) of the first propagating wave mode in the layered ground [4].

To demonstrate the effectiveness of a WIB, a concrete plate of 12 m width and 0.6 m thickness is placed on the lower half-space and is symmetric about the track centre-line. The Young's modulus, Poisson's ratio and density of the plate are 37.6 GN/m$^2$, 0.15 and 2400 kg/m$^3$. The depth from the ground surface to the upper face of the plate is 1.4 m. The cut-on frequency is calculated as about 15 Hz. The ground surface and the layer interface are each discretized using 60 three-noded BEs covering a lateral distance of 30 m from the track centre-line. The mesh is shown in Fig. 6. The length of each BE is 0.5 m. Vibration levels are predicted up to 50 Hz. At 50 Hz, the Rayleigh wavelength is $77/50 = 1.54$ m. In other words, each wavelength contains three elements at this frequency. For higher frequencies, a finer mesh is required. Half the plate cross-section (6 m wide) is meshed using 12 eight-noded quadrilateral FEs. The predicted velocity levels with the presence of the WIB are shown in Fig. 5 in thick lines.

Table 2
Parameters for a soft layered ground

| Layer | Depth (m) | Young's modulus ($10^6$ N/m$^2$) | Poisson's ratio | Density (kg/m$^3$) | Loss factor | P-wave speed (m/s) | S-wave speed (m/s) | Rayleigh wave speed (m/s) |
|---|---|---|---|---|---|---|---|---|
| 1 | 2.0 | 30 | 0.47 | 1550 | 0.1 | 340 | 81.1 | 77 |
| Half-space | | 360 | 0.49 | 2000 | 0.1 | 1755 | 245 | 233 |

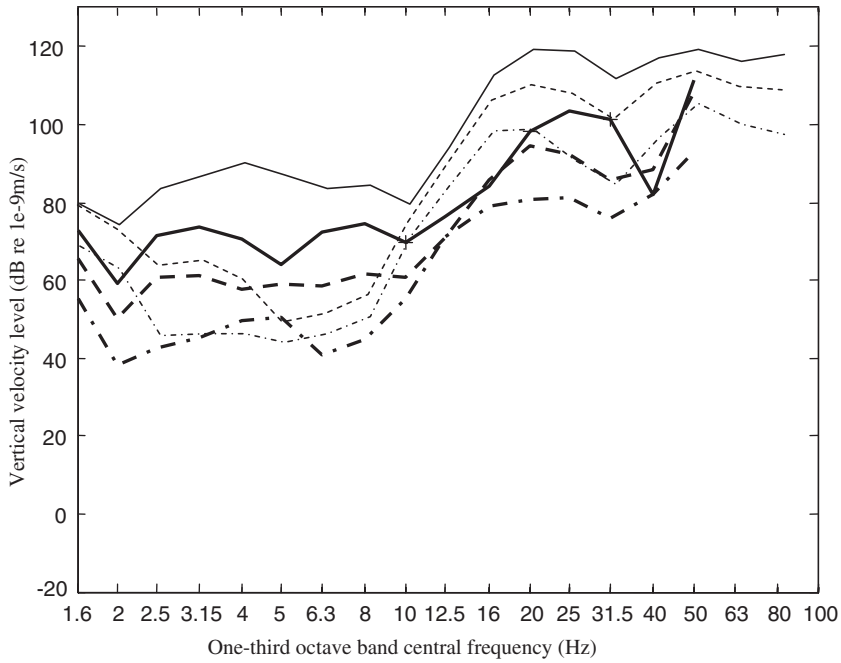


Fig. 5. Vertical velocity levels at 5 m (—), 10 m (– – –) and 20 m (– · –) from the track centre-line when a passenger coach runs at 60 m/s. Thin line, without WIB; Thick line, with WIB.

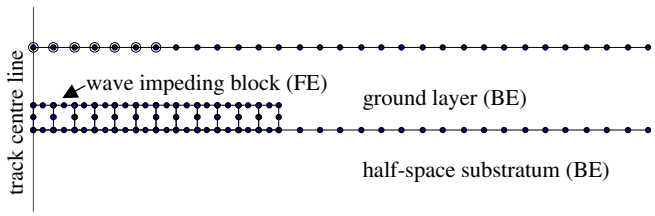


Fig. 6. Model for the WIB in the ground layer (track model attached at circled nodes).

At 5 m, the WIB provides more than 10 dB vibration reduction for all the frequencies considered. At 10 and 20 m a similar reduction is achieved in the 10 Hz and higher frequency bands but at lower frequencies in general there is overall a neutral effect with increases and decreases in different bands.

### 3.3. Ground vibration from underground trains

The third prediction case considered is a tunnel/track structure (Fig. 7). A slab track with UIC 54 rails and direct fasteners forms part of the invert of a concrete-lined, bored tunnel. The rail pads are relatively soft

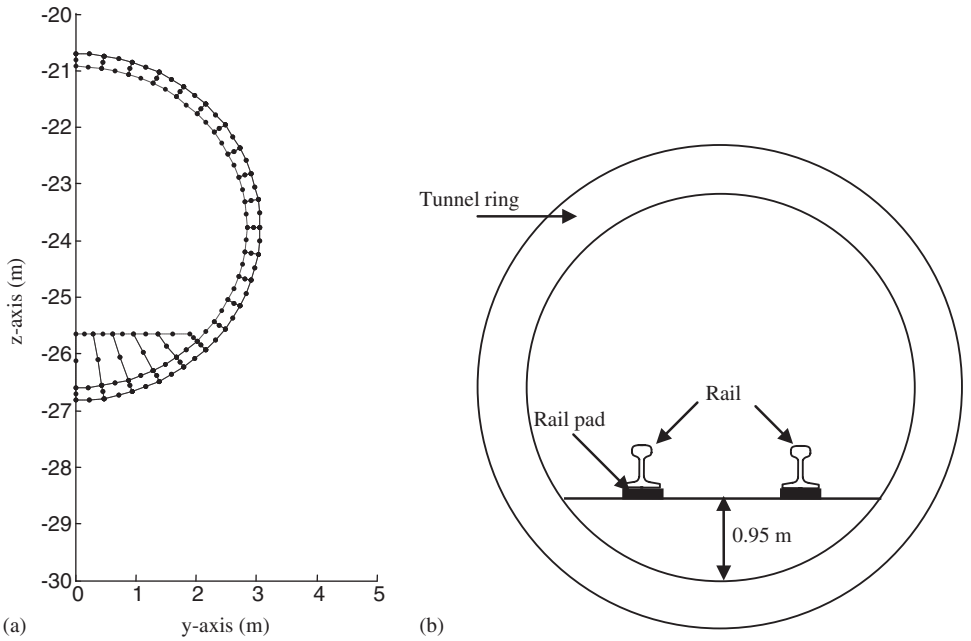


Fig. 7. Track/tunnel mesh (a) and cross-section diagram (b) for the tunnel.

Table 3
Parameters for the track (two rails)

| | |
|---|---|
| Mass of rail beam per unit length of track (kg/m) | 108 |
| Bending stiffness of rail beam ($N m^2$) | $9.55 \times 10^6$ |
| Loss factor of the rail | 0.01 |
| Rail pad stiffness per unit length of track ($N/m^2$) | $3.8 \times 10^8$ |
| Rail pad loss factor | 0.2 |

10 mm thick pads with a dynamic stiffness per pad of 125 MN/m. Parameters for the track model are listed in Table 3. The tunnel invert is 26.6 m below the ground surface. The tunnel ring inner radius is 2.84 m and its outer radius is 3.06 m. The ground is a deep drift of clay approximated as a homogeneous half-space with P-wave speed 1250 m/s, shear wave speed 230 m/s and density 2050 $kg/m^3$. For the FE/BE model, 80 three-noded BEs are used to model the ground surface covering a lateral distance of 40 m from the tunnel centre-line. At 200 Hz, each Rayleigh wavelength contains about four BEs. The FE mesh of eight-noded quadrilateral elements for the tunnel structure is also shown in Fig. 7. The rolling stock consists of 9 coaches (length 23 m, axle spacing 2.5 m and pivot spacing 16 m) and runs at 40 km/h (11.1 m/s). The unsprung mass of the powered axles is 844 kg and the unpowered axles, 795 kg. A mean rail roughness spectrum of a number of measurements of lines in the UK is assumed [21] in the absence of specific data.

The predicted vertical velocity level 7 m from the horizontal alignment on the ground surface and that for the tunnel crown are shown in Fig. 8 for one-third octave band centre frequencies from 16 to 200 Hz. Most of the vibration energy is distributed around the peak at 80 Hz at which the resonance of the unsprung mass on the track occurs. Vibration attenuation from the tunnel to the ground surface increases with frequency. Some measurements are also included in Fig. 8. These are of vibration on the floor slab at grade of a large building with piled foundations in clay ground similar to that modelled here. They are presented in order to demonstrate that the model produces levels of realistic magnitude but the lack of knowledge of parameters surrounding the measurement, not only the roughness, and the effect of the building in the measurements is

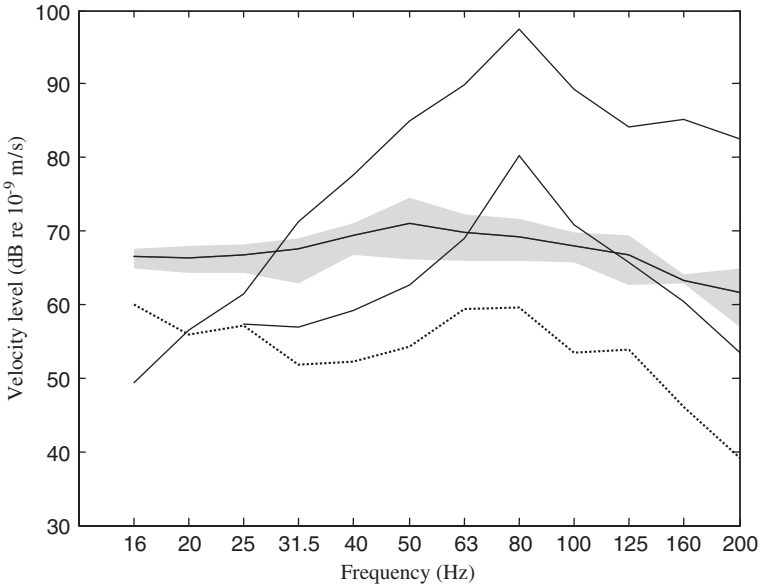


Fig. 8. Predicted velocity levels: -·-·-, at $y = 7$ m on the ground surface; – – –, at the tunnel crown; measured level at $y = 7$ m in the building at ground level: ——, mean with range shaded; ····· background vibration level.

such that the prediction and measurement do not necessarily agree well. A more specific comparison with measurements should be carried out in future work. In the meantime, the case serves as a demonstration that use of such models as prediction tools for environmental vibration requires enormous effort in terms of ground site characterization, and specific track, and structure parameters to be reliable.

## 4. Discussion

The three cases have been analysed using models with 100, 120 and 100 BEs in the largest BE domain. The first and second cases have second BE domains of half the number of elements and each case contains a FE domain with a small number of elements. The solution has been obtained in each case at 512 wavenumbers with a spacing of $0.05 \times 2\pi$ rad/m. This range of wavenumbers has been found to be sufficient to provide accurate results for ground vibration analyses with a wide range of soil parameters [12]. The computing times vary greatly depending on the total number of nodes in the model. As an example, a model with 100 BEs takes a few seconds for each wavenumber and about 15 min per frequency on a conventional 3 GHz, single processor, Windows PC. No attempt has been made in the coding to use highly efficient solution routines which may reduce times further. The memory requirement is small, being dominated in most cases by the space required to store the matrices for the largest BE domain. This is less than 6 Mb for each of the [**H**] and [**G**] matrices in double precision for 100 BEs.

While the model may be used with much greater numbers of elements for more complicated geometries than those of the examples, it is believed that these represent realistic practical analyses covering the frequency range for both 'whole body' vibration and ground-borne noise.

The method presented here is efficient in computational terms taking only a matter of minutes for the computation of surface vibration cases on a desktop personal computer and about 20 h for a spectrum result of the larger model for the tunnel case. A fully 3D coupled finite-element BE analysis of equivalent detail to the tunnel case has not been carried out but from experience of such models [22], would be expected to take at least 40 h per frequency on similar computing equipment. In practice, it is memory resources that limit (3D) BE analysis on a PC. It would require more than 2 Gbytes to store the system matrices of the equivalent 3D model.

The computing times are not small enough for very rapid design calculations but are practicable for environmental predictions and specific case analysis. However, this requires detailed, validated ground and structure parameters to be available.

## 5. Conclusions

A model based on the wavenumber finite and boundary element methods has been produced for predicting ground vibration from trains running either on the ground surface or in tunnels. This model requires the ground and built structures to be homogeneous in the track direction but allows an arbitrarily shaped cross-section. The usefulness of the model is demonstrated by predictions for three different engineering cases: surface vibration at a location with an embankment, the reduction of vibration affected by a wave impeding block and vibration from trains running in tunnels. In the case of the embankment, the model is shown to be accurate by comparison with measurement data even though specific roughness data have not been available. The computing resources required are reasonable for practical analyses and predictions of real cases.

## Acknowledgements

This work is supported by the Engineering and Physical Sciences Research Council of the UK under Research Grant GR/R67309/01, Ground vibration and noise from trains in tunnel. The measurement data from Via Tedalda were used with the kind permission from the authors of Ref. [19].

## References

[1] P. Grootenhuis, Floating track slab isolation for railways, *Journal of Sound and Vibration* 51 (1977) 443–448.
[2] H. Grundmann, M. Lieb, E. Trommer, The response of a layered half-space to traffic loads moving along its surface, *Archive of Applied Mechanics* 69 (1999) 55–67.
[3] V.V. Krylov, Generation of ground vibrations by superfast trains, *Applied Acoustics* 44 (1995) 149–164.
[4] X. Sheng, C.J.C. Jones, D.J. Thompson, A theoretical model for ground vibration from trains generated by vertical track irregularities, *Journal of Sound and Vibration* 272 (2004) 937–965.
[5] D. Clouteau, M. Arnst, T.M. Al-Hussaini, G. Degrande, Freefield vibrations due to dynamic loading on a tunnel embedded in a stratified medium, *Journal of Sound and Vibration* 283 (2005) 173–199.
[6] C.J.C. Jones, D.J. Thompson, M. Petyt, A model for ground vibration from railway tunnels, *Proceedings of the Institution of Civil Engineers—Transport* 153 (2002) 121–129.
[7] L. Andersen, C.J.C. Jones, Vibration from a railway tunnel predicted by coupled finite element and boundary element analysis in two and three dimensions, in: H. Grundman, G.I. Schuëller (Eds.), *Structural Dynamics—EURODYN'2002*, Balkema, Lisse, 2002, pp. 1131–1136.
[8] D. Aubry, D. Clouteau, G. Bonnet, Modelling of wave propagation due to fixed or mobile dynamic sources, in: N. Chouw, G. Schmid (Eds.), *Wave Propagation and Reduction of Vibrations*, Berg-Verlag, Bochum, 1994, pp. 109–121.
[9] H. Takemiya, S. Yuasa, Lineside ground vibration induced by high-speed trains and mitigation measure WIB, in: L. Frýba, J. Náprstek (Eds.), *Structural Dynamics—EURODYN'99*, Balkema, Rotterdam, 1999, pp. 821–826.
[10] L. Gavric, Computation of propagative waves in free rail using a finite element technique, *Journal of Sound and Vibration* 185 (1995) 531–543.
[11] L. Gavric, Finite element computation of dispersion properties of thin-walled waveguides, *Journal of Sound and Vibration* 173 (1994) 113–124.
[12] X. Sheng, C.J.C. Jones, D.J. Thompson, Modelling ground vibration from tunnels using wavenumber finite and boundary element methods, *Royal Society*, *Proceedings A*, Published on-line, June 2005.
[13] J. Dominguez, *Boundary Elements in Dynamics*, Elsevier Applied Science, London, 1993.
[14] A.J.B. Tadeu, E. Kausel, Green's functions for two-and-a-half-dimensional elastodynamic problems, *Journal of Engineering Mechanics* 126 (2000) 1093–1097.
[15] X. Sheng, C.J.C. Jones, D.J. Thompson, Moving Green's functions for a layered circular cylinder of infinite length, ISVR Technical Memorandum 885, University of Southampton, 2002.
[16] P.R. Johnston, B.M. Johnston, A simple device to improve the accuracy of evaluating weakly singular boundary element integrals, *Communications in Numerical Methods in Engineering* 18 (2002) 189–194.
[17] K.M. Singh, M. Tanaka, On non-linear transformations for accurate numerical evaluation of weakly singular boundary integrals, *International Journal for Numerical Methods in Engineering* 50 (2001) 2007–2030.
[18] C.J.C. Jones, D.J. Thompson, M. Petyt, Ground-borne vibration and noise from trains: Elasto-dynamic analysis using the combined boundary element and finite element methods, ISVR Technical Memorandum No. 844, University of Southampton, 1999.

[19] C.G. Lai, A. Callerio, E. Faccioli, A. Martino, Mathematical modelling of railway-induced ground vibrations, in: N. Chouw, G. Schmid (Eds.), *Proceedings of the International Workshop Wave 2000*, 2000, pp. 99–110.
[20] X. Sheng, C.J.C. Jones, D.J. Thompson, A comparison of a theoretical model for quasi-statically and dynamically induced environmental vibration from trains with measurements, *Journal of Sound and Vibration* 267 (2003) 621–635.
[21] A.E.J. Hardy Draft proposal for noise measurement standard for ERRI committee C163, Report RR-SPS-97-012 of AEAT Rail Ltd., Published through European Rail Research Institute, 1997.
[22] L. Andersen, C.J.C. Jones, Coupled boundary and finite element analysis of vibration from railway tunnels—a comparison of two- and three-dimensional models, *Journal of Sound and Vibration*, this volume (doi:10.1016/j.jsv.2005.08.044).